Final Report
A New Log Evaluation Method to Appraise Mesaverde Re-Completion Opportunities
Grant
DE-FG2601NT15264

Prepared for:
NETL AAD Document Control Bldg. 921
U.S. Department of Energy
National Energy Technology Laboratory
P.O. Box 10940
Pittsburgh, PA 15236-0940

Prepared by:

Benson-Montin-Greer Drilling Corporation
4900 College Blvd.
Farmington, NM 87402

For the period Sept. 12, 2001 through Sept. 11 2003

Abstract

Artificial intelligence tools, fuzzy logic and neural networks were used to evaluate the potential of the behind pipe Mesaverde formation in BMG's Mancos formation wells. A fractal geostatistical mapping algorithm was also used to predict Mesaverde production. Additionally, a conventional geological study was conducted. To date one Mesaverde completion has been performed. The Janet #3 Mesaverde completion was non-economic. Both the AI method and the geostatisical methods predicted the failure of the Janet #3. The Gavilan #1 in the Mesaverde was completed during the course of the study and was an extremely good well. This well was not included in the statistical dataset. The AI method predicted very good production while the fractal map predicted a poor producer.

Table of Contents

Introduction and Executive Summary

BMG is small oil company operating in the San Juan Basin of New Mexico. The company employs 20 people to operate 130 wells. As operator of the Gavilan and West Puerto Chiquito units, BMG serves as spokesman for the forty different working interest owners and twice that many royalty and overriding interests owners in the units. In effect the unit serves as a consortium of entities with interest in this research project.

Oil and gas is produced from the Mancos formation in the Gavilan and West Puerto Chiquito units. The focus of this research project is the Mesaverde formation above the Mancos formation. During the time the Mancos wells were drilled, production from the Mesaverde was believed to be non-economic and little effort was expended in evaluating the Cliff House, Menefee, and Point Lookout intervals in the Mesaverde. Recently an offset operator developed Mesaverde production. The new production created interest in behind pipe potential of the Mancos wells. The information needed to evaluate the Mesaverde formation is limited to the existing logs that were collected at the time of the Mancos development. The suite of logs run through the Mesaverde during the Mancos development period is not uniform. One core cut by BMG during this time period indicated that the three intervals in the Mesaverde formation were saturated with water and non-productive.

The intention of this study is to use new log evaluation methods based on artificial intelligence to evaluate the potential of behind pipe production in the Mesaverde formation for wells in the Gavilan and West Puerto Chiquito units. The approach is to use modern logs coupled with the Mesaverde production history of new wells drilled outside BMG operated units to develop correlations that can be used to predict the Mesaverde producing rate of wells within the units.

During the first year of this two year project, data consisting of logs and available production reports from 35 wells were acquired and reviewed. Generally gamma ray logs, density porosity logs or bulk density logs, plus a deep resistivity log were available through the Mesaverde section for all 35 wells. Production histories of nine Mesaverde wells were available from the NM State productions records. The initial producing rate from these wells in the study area was used to correlate with log parameters. The initial producing rate of the nine wells is the average barrels equivalent oil produced per day (Bepd). Bepd is defined as the barrels of oil per day plus the average mcf of gas produced per day divided by six. The average is based on the first 12 producing months for each well.

The Cliff House, Menefee, and Point Lookout intervals were identified on the digitized logs. A crossplot of the gamma ray log versus the porosity difference was developed and the resulting pattern was useful for visually differentiating good wells from bad wells. The porosity difference axis on the plot requires the calculation of both neutron and density porosities, but unfortunately neutron logs were not run in most wells in BMG operated units. Nevertheless, the patterns observed in the crossplots of gamma ray versus density porosity alone proved useful. In a similar manner a crossplot of gamma ray versus pseudo-water saturation displayed interesting patterns. Visually the patterns displayed in both crossplotting techniques seemed to correlate with the initial producing rate. A statistical method was developed to characterize the visual patterns that enabled a numerical correlation with production. Correlations were obtained for

hydrocarbon production, but unfortunately an adequately trained neural network could not be found for water production.

The statistics used to describe the patterns served as input to a neural network with the initial production as the output. The network was limited to a simple architecture due to the limited number of wells with production history (9 wells). Correlations between the log patterns and production were developed. These correlations were used to predict production from the behind pipe Mesaverde formation in the BMG operated units. The hydrocarbon correlations can be applied to any well with the Mesaverde section behind pipe provided the provided the gamma ray and density logs are available. Unfortunately correlations based on resistivity logs proved to be unreliable, perhaps due to changes in connate water resistivity. Correlations Company, located in Socorro NM, can apply the trained neural network to provide any operator with hydrocarbon rate predictions given the gamma ray and density logs. The data provided in the report can be used by any operator to train a neural network and make proprietary predictions.

During the contract period data became available from the completion of the Mesaverde zone in the NM&O Gavilan #1 well. This well has produced ~1mmcf/day (180 Bepd) for 1 year. The conventional analysis of BMG wells near this remarkable well suggested that the nearby Janet #3 was a Mesaverde completion opportunity. The Janet #3 is located updip from the San Juan Basin Blanco Pool producing from the Mesaverde, but it is downdip from the NM&O Gavilan #1 well. The Mesaverde interval in the Janet #3 exhibits neutron-density log gas crossover effect, and favorable deep resistivity properties.

A fractal geostatistical algorithm was used to map the spatial distribution of Mesaverde production in the study area. Both the neural network and the fractal map predicted the Janet #3 to be a poor well as confirmed by a non-commercial completion. The neural network predicted the Gavilan #1 to be a good Mesaverde well while the fractal map suggested that it was a poor completion target.

***Experimental Data* - Structure of the dataset in the study area**

Digitized logs from thirty-five wells make up the study area dataset. Name and API number in Table I identify the wells. Inspection of Table I shows that gamma ray, some type of density measurement, and deep resistivity are available for most logs in the dataset. Ten wells in the dataset are completed in the Mesaverde section. Eight wells were used to develop correlations between log properties and the initial producing rate. The initial producing rate is defined as the average daily rate for the first 12 producing months.

Typical logs

A typical log suite is shown in Fig. 1 with the Jicarilla G (6A) logs. The presentation of the logs is not typical of the format used by the logging companies. All logs in Fig. 1 are shown in $\log_{10}$ values. This is somewhat confusing especially when viewing the gamma ray and caliper logs. Notice that a gas crossover effect accompanied by clean gamma ray and favorable resistivity is especially evident at ~5500 ft.

The objective of the study is to find patterns in the logs that relate to the initial producing rate from the well. The three logs that best relate to production were identified with crossplots that are discussed next.

***Results and Discussion* - Patterns in well log crossplots**

The coupling of well known neutron-density log crossover with the gamma ray log in a crossplot format was examined for patterns that might relate to the initial producing rate. The crossover phenomenon occurs when hydrocarbons replace water in the pore space. This causes the density log to read higher porosity and the neutron to read lower porosity. Normally the neutron log reads slightly higher porosity than the density. Where the two logs crossover it is a strong indicator of gas and in some cases oil. With this background, the difference between the neutron porosity and the density porosity is less than 0.0 when hydrocarbons are present. Thus, a crossplot of the gamma ray log versus the porosity difference log should point out intervals that have clean sand and the presence of gas. Shown in Fig. 2 is a crossplot constructed with Jicarilla (6A) data. Notice that the red data points (Cliff House interval) show that Cliff House has about 16

data points where the gamma ray is less than 100 units and the porosity difference (Φ_N-Φ_D) is less than zero. Since the Jicarilla (6A) is a good well (563Mcf/d, 94 Bepd), there could be a relationship between the plot pattern and the well's production. A similar pattern was observed in the porosity difference crossplots prepared with datasets from the other wells as shown in Fig. 3. The top two plots are considered to be good wells (greater than 100 Mcf/d, 17 Bepd) while the bottom two are considered as poor wells (less than 100 Mcf/d, 17 Bepd). The good wells show clean gamma ray with crossover. This trait is much less evident in the poor wells.

Unfortunately, the neutron porosity log is not included in all well log suites. Recognizing that most log suites include a gamma ray, bulk density or Φ_D and deep resistivity logs in the dataset, various crossplot combinations of these logs were evaluated for patterns. Using a pseudo-water saturation value produced patterns similar to density difference logs. The function does not include the values for Rw or porosity required by Archie's equation. There are multiple reported values for Rw through out the Mesaverde formation and density porosity is not an indicator of true porosity because of the previously discussed hydrocarbon effect. The pseudo-water saturation is defined as:

$$1/\sqrt{Rt} / RhoB$$

Rt is the value, ohmmeters, of the deep resistivity log and RhoB is the value, gm/cc, of the bulk density log. This quantity produced useful patterns when plotted versus the gamma ray log as shown in Fig 4. In the case of Jicarilla (6A) it appears that both the Point Look Out interval and the Cliff House interval contain data points with less than 100 gamma ray units and a pseudo-water saturation value less than 0.1. The Jicarilla (6A) well was defined as a good producer.

Similar patterns were observed in the other wells as shown in Fig. 5. Again the top two plots are considered good wells while the lower two are poor wells. The differences in the plots are apparent. Statistical properties of the individual logs were used to define the patterns observed in the gamma ray versus pseudo water saturation crossplot and the gamma ray versus porosity difference logs.

Goodness of the statistical properties of the logs

Eight wells had Mesaverde production plus the logs required to construct Figs. 2 & 3. The statistical properties sum, average (avg), and standard deviation (STD) of the perforated interval of each of the logs were calculated. The perforated interval is reported in public domain State records as approximately the top of the Mesaverde to the top of the Mancos. The statistical properties of the logs through the perforated interval are shown in Table II along with the initial producing rate and the fuzzy rank.[1] Fuzzy ranking was used to prioritize the statistical properties for use in a neural network.

Fuzzy curves were constructed with the data shown in Table II. Two of the top ranked fuzzy curves are shown in Fig. 6. All values shown on the curve are normalized between 0-1. A de-normalized fuzzy rate versus the average values of the gamma ray graphs is shown in Fig. 7. The graph includes seven data points used to construct the continuous fuzzy curve shown on the graph. Note that the production rate is inversely proportional to the average gamma ray value. (Recall that the dataset includes the gamma ray measurements from top to bottom of the Mesaverde). The ranking of the statistical properties sum, average, and standard deviation was calculated by adding the range of the fuzzy curves to the R^2 value of the best-fit line to the data points.

In a similar manner, the initial production rate versus the sum of the bulk density was used to construct the fuzzy curve shown in Fig. 8. Again the de-normalized fuzzy curve includes the values used to construct the fuzzy curve.

Neural network correlations

The eight wells used to develop the neural network correlations which were used to predict the performance of BMG wells with behind pipe Mesaverde potential are:

Ribeyowids Fed. #16	Ruddock #7
Divide #1	Florance Federal #7
Gavilan #2	Jicarilla 96 #6A
Elk Com 1A	Jicarilla 96 #7[a]

Only a simple neural network architecture can be used to develop correlations between the statistical properties and the initial production rate due to the limited number of study area records[2] (wells with Mesaverde production history). Hence the architecture

is limited to two inputs in one hidden node. The linearity of the fuzzy curves supports using the simple network. With production as the output, four networks with various combinations of inputs were tested. The best training results were obtained with the standard deviation (STD) of the gamma ray log as one input and the average (Avg) of the bulk density log as the other. This 2-1-1 neural network trained to 96% as shown in Fig.9.

Recently the 1st year's production from a newly completed Mesaverde well (Gavilan #1) became available. The information from the NM&O Gavilan #1 serves as a blind test prediction of the neural network shown in Fig. 9. Raster images of the NM&O Gavilan #1 well logs were obtained and digitized. The well produced an average of 1.1 mmcf/d or 180 Bepd during 2002. This very high rate is outside the range of the production data used to develop the neural network shown in Fig. 9. Nevertheless given the STD of the gamma ray log and the Avg of the bulk density log through the Mesaverde section of the NM&O Gavilan #1, the Fig. 9 network predicts that the well will produce 550 mcf/d or 92 Bepd. The prediction is noted on the graph with the large open circle. The trained neural network was used to forecast Mesaverde Completions in the 18 wells shown in Table III. The predictions are based on a public domain neural network used by Correlations Company that was downloaded from the web.[3]

During the study it became apparent that an inverse correlation existed between the thickness of Point Lookout in the Mesaverde and the initial producing rate from the Mesaverde. The correlation is shown in Fig. 10. and is based on public domain picks of the top of the Mancos. The thickness information comes from the Gavilan 2, the Florance 7, the Ruddock 7, the Divide 1, the Ribeyowids 2, the Elk Com 1A, and the Jicarilla 6, 7, & 8 wells. It should be noted that the Mancos tops in the public domain are problematic. For example, the NM&O Gavilan #1 Point Lookout thickness appears to be 138 ft, yet the state well file database reports it as 318 ft.

An attempt to apply the same fuzzy ranking/neural network technology to water production records was unsuccessful perhaps due to the variation in the reported connate water resistivity. The statistics of a combination of gamma ray and deep resistivity logs were evaluated, but none were found that would correlate water production with the patterns seen in the logs. A neural network architecture was not found that would train and predict water production.

The fuzzy ranking/neural network technology used in this study is essentially statistical in nature. Geostatistical methods were applied to the same dataset in an effort to confirm the artificial intelligence results. The state well file database is the source for well locations and formation tops. The Point Lookout depths are believed to be the most dependable of the available records. A Point Lookout structure map is shown in Fig. 11.

The convergence of the contour lines in the NE quadrant of the map suggests the presence of a fault. The Jicarilla G6, H7, and 8A wells are located near the fault and all were good producers as seen in Table I and II.

Fractals are believed to model the spatial distribution of coast lines and have been used to map reservoir properties. A geostatistical fractal mapping algorithm was used to map the Mesaverde production in the study area. The fractal map as shown in Fig. 12 was generated without knowledge of the NM&O Gavilan #1 well. Shown as a large circle at the approximate center of Fig. 12 is the location of the Janet # 3 well. The fractal mapping algorithm supports the neural network prediction that the well is a poor Mesaverde producer.

The fractal distribution of the neural network predicted production is shown in Fig. 13. The large circle at the approximate center of Fig. 13 is the location of the NM&O Gavilan #1 well. Clearly the fractal mapping technique failed to predict the production from this extremely good well, whereas the neural network predicted a good well.

Visually the Janet #3 does not fit the patterns of the other wells shown in Fig. 14. The poor Ribeyowids well has no crossover with clean gamma ray while the Janet well does. The neural network predicted Janet #3 to be a poor well, which was confirmed with a non-commercial completion.

Shown in the gamma ray versus crossover plots in Fig. 15 is a comparison of a poor well and two good wells with the extremely good NM&O Gavilan #1. The pattern of clean gamma ray with crossover is evident in the Gavilan #1. The neural network predicted the Gavilan #1 to be a good well.

Field Results

After 3 months in 2003 of producing water the Janet #3 Mesaverde completion was finalized as a non-economic producer. The completion attempt was based on following geologic findings:

- Janet #3 is located updip from San Juan Basin Mesaverde Blanco Pool.
- it is downdip from the NM&O Gavilan #1 well.
- the Mesaverde interval in the Janet #3 exhibits neutron-density log gas crossover effect.
- the deep resistivity log properties are favorable.

Additionally, production from the Mancos had declined to marginal economic status. The $130,000 Janet #3 completion was non-commercial. Additional Mesaverde completions will be attempted in the future.

Conclusions

A conventional geologic study resulted in a non-commercial Mesaverde completion in the Janet #3. A neural network with the standard deviation of the gamma ray log and the average of the bulk density log as inputs was trained with production data from producing Mesaverde wells in the study area. The trained neural network predicted a non-commercial completion in Janet #3.

The same network predicted that the NM&O Gavilan #1 well would be a good well. The network succeeded despite the Gavilan #1's producing rate exceeding the limits of the neural network training dataset. The trained neural network used to make these predictions is available through Correlations Company, located in Socorro NM, or the information in Table II can be used to develop an in-house proprietary neural

network. In addition to commercial neural networks, public domain[3,4] neural networks are available on the web.

Attempts to develop a neural network to predict water production were not successful. The training correlations were too low to be used to make predictions.

A fractal geostatistical mapping algorithm was used to map the Mesaverde production in the study area. The geostatistical map identified both the Janet #3 and the Gavilan #1 as poor producers.

References:

1. Weiss, W. W., Wo, S., Weiss, J.: "Data Mining at a Regulatory Agency to Forecast Waterflood Recovery," SPE 71057 Presented at the 2001 SPE Rocky Mountain Technical Conference, Keystone CO, 21-23 May 2001.
2. Du, Y., Weiss, W.W., Xu, J., Balch, R.S., and Li, D.:"Obtain an Optimum Artificial Neural Network Model for Reservoir Studies," Paper 84445 presented at the SPE Annual Conference, Denver, CO 5-8 October 2003.
3. www-ra.informatik.uni-tuebingen.de/SNNS/
4. www.npto.doe.gov/Software/

Table I Data Base								
~1BCFG Cum Prod Wells								
API #	Well Name	Mcf/D	Log Suite					
30039062000000	E34 3	163	Not Received					
30039211650000	JICARILLA-G 6-A	563	GR_1	NPHI_1	DPHI_1			RHOB_1
30039212360000	JICARILLA H 7-A	636	GR_1				DRHO_1	RHOB_1
30039212730000	JICARILLA-H 8A	324	GR_1	NPHI_1	DPHI_1		DRHO_1	RHOB_1
30039221240000	RUDDOCK 7	383	GR_1	NPHI_1			DRHO_1	RHOB_1
30039221250000	FLORANCE 7-A	489	GR_1					RHOB_1
~1/4-3/4 BCFG Cum Prod Wells								
30039202720000	TAPACITO 1	67	GR_1		DPHI_1		DRHO_2	interrupted
30039240440000	DAVIS FED COM 15	610	Not Received					
Uneconomic (Dry Holes)								
30039228300000	DIVIDE 1	7	GR_1		DPHI_1		DRHO_1	RHOB_1
30039233120000	GAVILAN-HOWARD 1	21	interrupted		interrupted		interrupted	interrupted
30039233670000	GAVILAN 2	75	GR_1	NPHI_1		DNPI_1	DRHO_1	RHOB_1
New Wells								
30039262840000	Elk Com 1A	257	GR		DPHI			
30039235540000	Ribeyowids Federal 2 #16	4	GR	NPHI	DPHI			
Candidate Wells								
30039203250000	CANADA OJITOS UNIT 14		GR_1		DPHI_1		DRHO_1	RHOB_1
30039228130000	CANADA OJITOS UNIT 23(N-22)		GR_1	NPHI_1	DPHI_1			RHOB_1
30039228140000	CANADA OJITOS UNIT 21(G-32)		GR_1	NPHI_1	DPHI_1		DRHO_1	RHOB_1
30039228370000	EMERALD 1		GR_1	NPHI_1			DRHO_1	RHOB_1
30039231850000	E.T. 1		GR_1	NPHI_1	DPHI_1		DRHO_1	RHOB_1
30039233070000	NATIVE SON 2		GR_1	NPHI_1	DPHI_1		DRHO_1	RHOB_1
30039235520000	CANADA OJITOS UNIT 26(K-31)		GR		DPHI			
30039235530000	CANADA OJITO 25 (B-32)		GR_1	NPHI_1	DPHI_1		DRHO_1	RHOB_1
30039235860000	HOMESTEAD RANCH 2		GR_1	NPHI_1		DNPI_1		RHOB_1
30039236050000	MOTHER LODE 2		GR	NPHI	DPHI			
30039236140000	NATIVE SON 3		GR_1	NPHI_1	DNPI_1		DRHO_1	RHOB_1
30039237670000	LODDY 1		GR_1	NPHI_1	DPHI_1		DRHO_1	RHOB_1
30039238070000	BEEKS BABBIT 1		GR_1	NPHI_1	DPHI_1		DRHO_1	RHOB_1
30039238300000	CANADA OJITOS 28(B-29)		GR_1			DNPI_1	DRHO_1	RHOB_1
30039238530000	FULL SAIL 3		GR_1 min= -186	NPHI_1	DPHI_1		DRHO_1	RHOB_1
30039238580000	JANET 3		GR_1	NPHI_1	DPHI_1		DRHO_1	RHOB_1
30039238670000	LADY LUCK 1		GR_1 min= -98	NPHI_1	DPHI_1		DRHO_1	RHOB_1
30039238740000	CANADA OJITOS 29		GR_1			DNPI_1	DRHO_1	RHOB_1
30039239090000	CANADA OJITOS UNIT 31		GR_1			DNPI_1	DRHO_1	RHOB_1
30039239850000	CANADA OJITOS UNIT 32		GR_1			DNPI_1	DRHO_1	RHOB_1
30039240500000	HIGH ADVENTURE 2		GR_1	NPHI_1	DPHI_1		DRHO_1	RHOB_1
30039240510000	HIGH ADVENTURE 1		GR_1	NPHI_1		DPHI_1	DRHO_1	RHOB_1
30039245050000	CANADA OJITOS UNIT 43		GR_1					RHOB_1
30039267890000	COYOTE 9 No.2		Not Found					
30039268100000	COYOTE COM 9		Not Found					

Table II Fuzzy Ranking										
Well		Jic 6A	Jic 7A	Jic 8A	Rud 7	F F 7	Div 1	Gav 2	Range	Goodness
	Mcf/d	563	636	324	383	489	7	75		
Log	GR									
Avg		140.7	126.7	77.4	69.6	82.3	45.3	43.1	0.64	1.63
STD		31.7	48.0	16.8	20.5	23.0	7.3	11.2	0.64	1.64
Sum x 1000		149.8	130.7	78.3	9.7	13.5	1.2	1.4	0.53	1.50
Log	RhoB									
Avg		2.53	2.46	2.42	2.44	2.49	2.48	2.44	0.22	1.09
STD		0.11	0.17	0.21	0.07	0.04	0.01	0.02	0.42	1.27
Sum		2691	2539	2445	342	409	65	78	0.45	1.41
Log	LLD									
Avg		23.5	18.4	20.5	43.2	34.0	31.8	41.4	0.36	1.3
STD		11.2	7.0	8.7	14.6	11.8	5.7	5.8	0.36	1.2
Sum x 1000		25.0	19.0	20.7	6.1	5.6	0.8	1.3	0.46	1.4
Log	Pseudo									
Avg		0.09	0.10	0.10	0.00	0.07	0.07	0.94	0.51	1.34
STD		0.01	0.02	0.02	0.00	0.01	0.01	0.12	0.51	1.30
Sum		92.0	102	98	0.33	12	2	30	0.41	1.30

Table III Neural Network Predictions			
Well	Predicted Production mcf/d	Map Location No.	Location Description T R Sec Unit
Canada Ojitos Unit #14	79	7	25N 1W S34 Unit C
Canada Ojitos Unit #21 (G-32)	538	30	26N 1W S32 Unit G
Canada Ojitos Unit #25 (B-32)	485	6	25N 1W S32 Unit B
Canada Ojitos Unit #28 (B-29)	536	13	25N 1W S29 Unit B
Canada Ojitos Unit #29 (K-31)	561	25	25N 1W S6 Unit E
Canada Ojitos Unit #31	559	29	26N 1W S31 Unit N
Canada Ojitos Unit #32	560	26	25N 1W S6 Unit J
Canada Ojitos Unit #43	541	34	26N 1W S8 Unit H
E.T. #1	1	10	25N 2W S28 Unit C
Native Son #2	33	11	25N 2W S27 Unit N
Native Son #3	263	3	25N 2W S33 Unit I
Homestead Ranch #2	1	4	25N 2W S34 Unit N
Loddy # 1	510	14	25N 2W S20 Unit F
Beeks Babbit #1	57	17	25N 2W S17 Unit G
Janet #3	3	15	25N 2W S21 Unit E
Lady Luck #1	34	1	25N 2W S5 Unit A
High Adventure #1	525	19	25N 2W S8 Unit H
High Adventure #2	560	18	25N 2W S9 Unit M
Training Wells			
	Actual , mcf/d		
Jicarilla-G6-A	563		26N 3W S2 Unit E
Jicarilla-H7-A	636		26N 3W S1 Unit D
Jicarilla-H8-A	324		26N 3W S12 Unit D
Ruddock 7	383		25N 3W S3 Unit E
Florance 7-A	489		25N 3W S4 Unit H
Divide 1	7		26N 2W S35 Unit H
Gavilan 2	75		25N 2W S26 Unit J
Elk Com 1-A	257		25N 2W S10 Unit D
Ribeyowids Federal 2 #16	4		25N 2W S2 Unit P

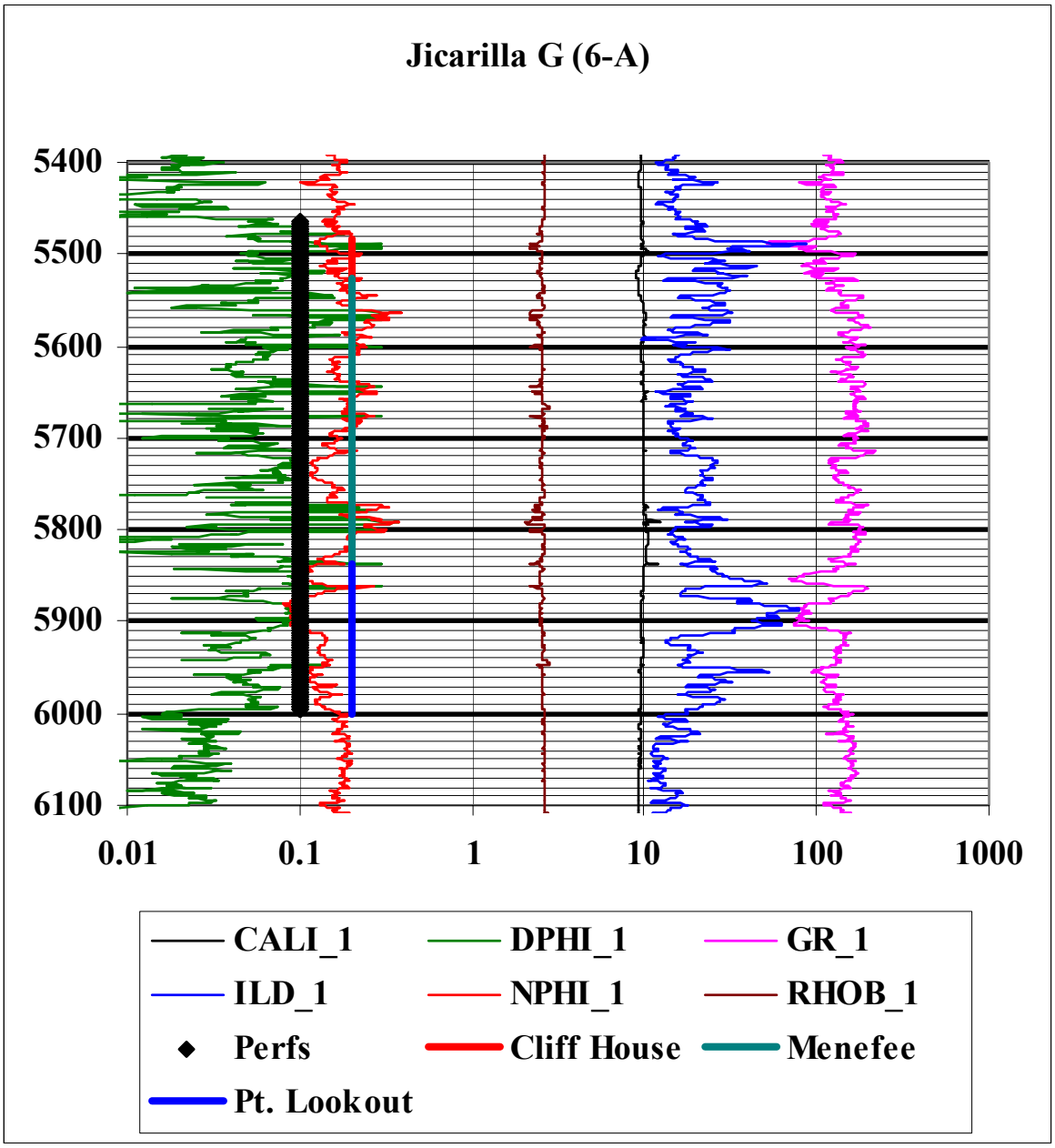

Figure 1. Typical Logs.

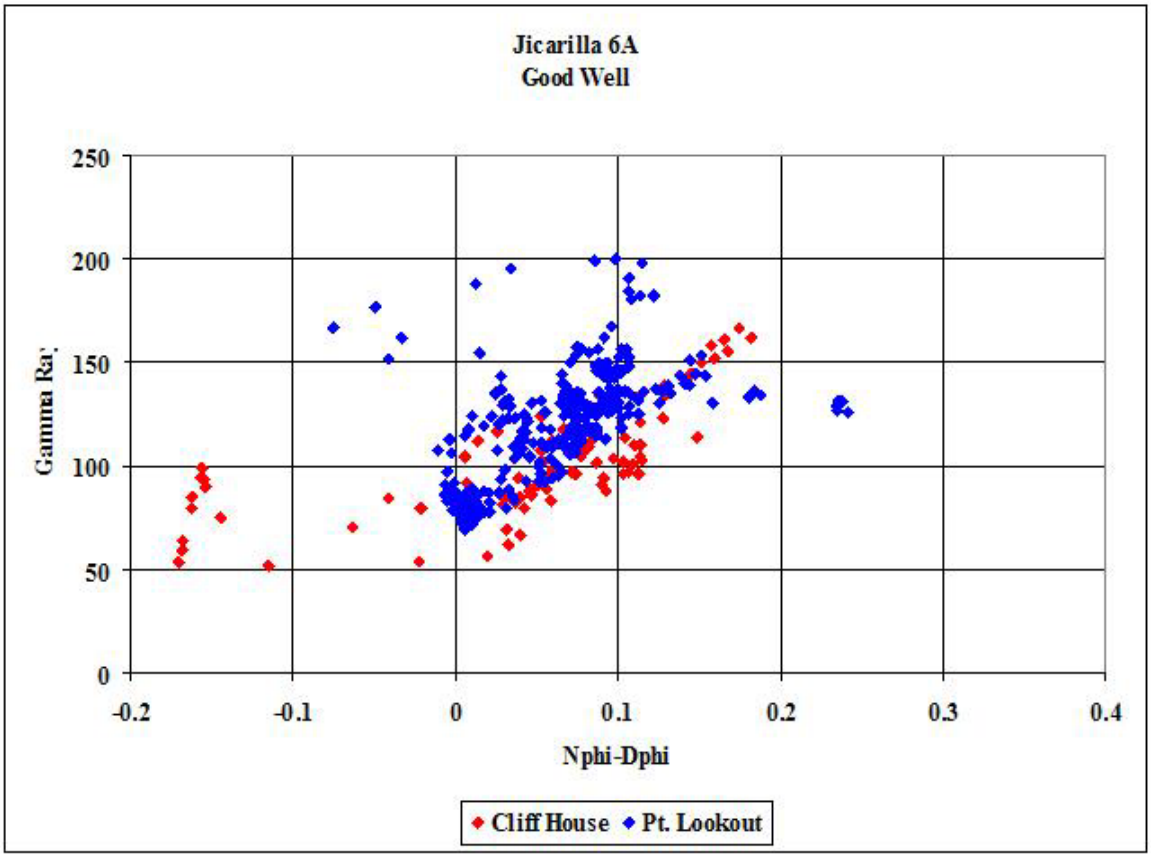

Figure 2. Gamma ray versus porosity difference crossplot.

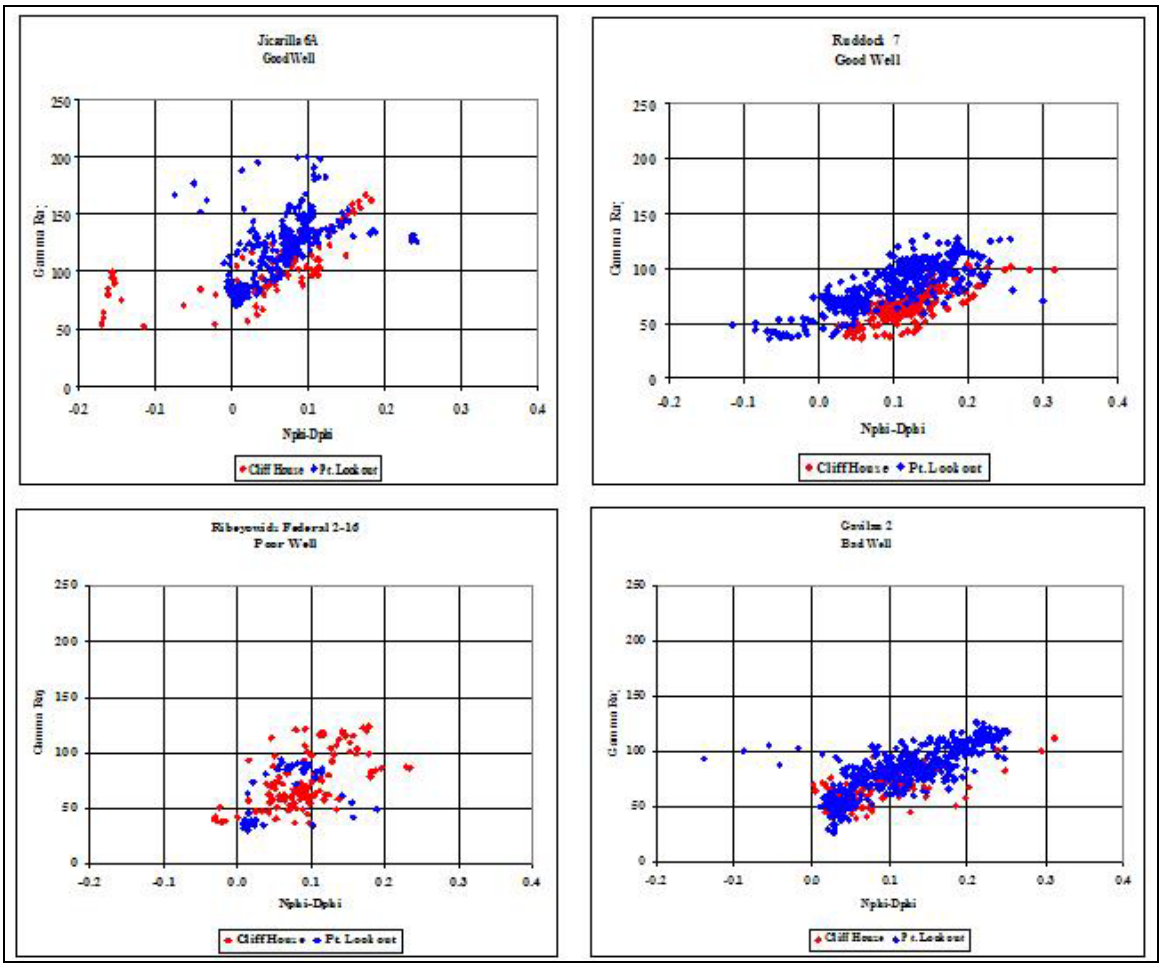

Figure 3 Gamma ray vs. porosity difference crossplots.

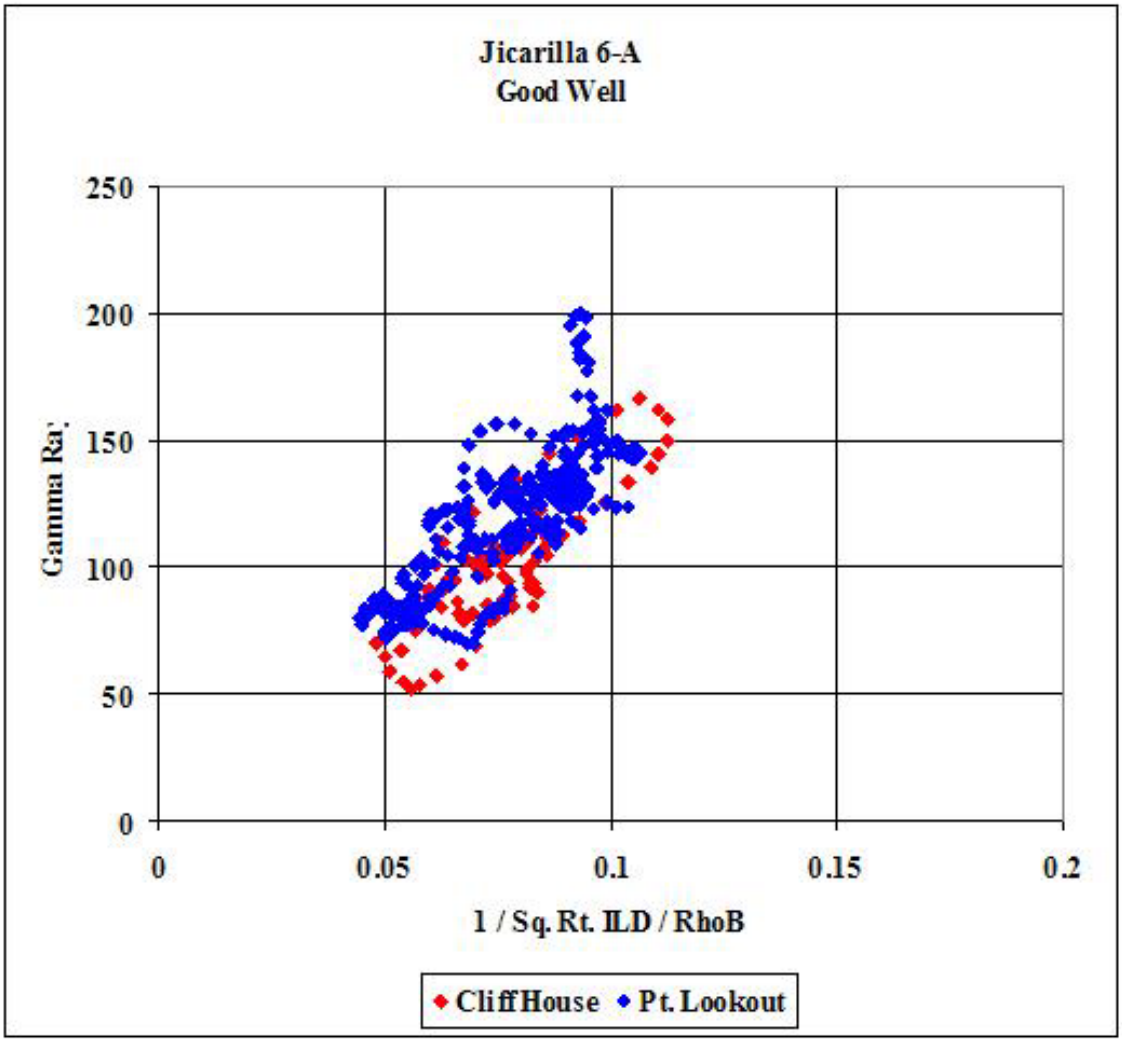

Figure 4. Gamma ray versus pseudo-water saturation.

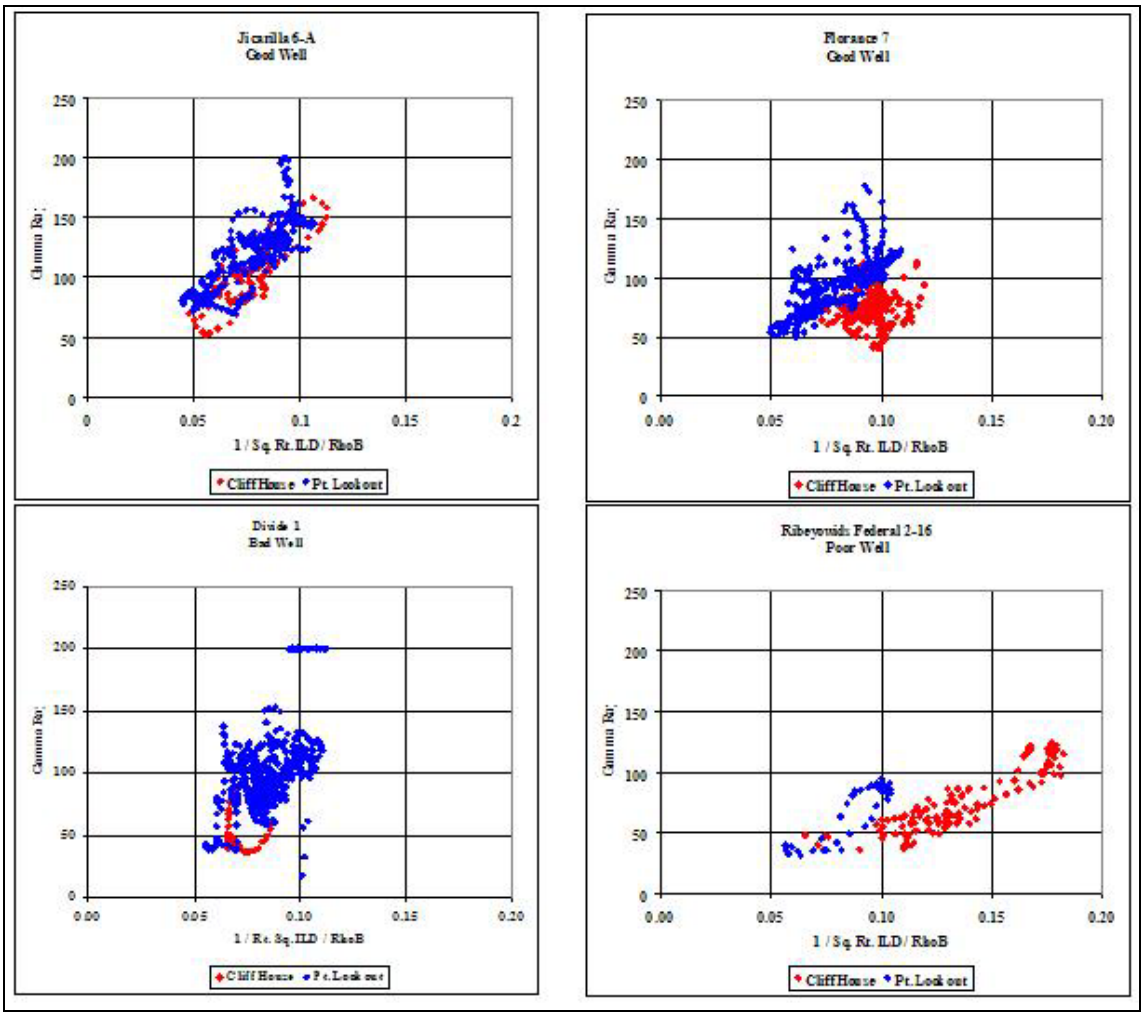

Figure 5 Gamma ray vs pseudo-log crossplots

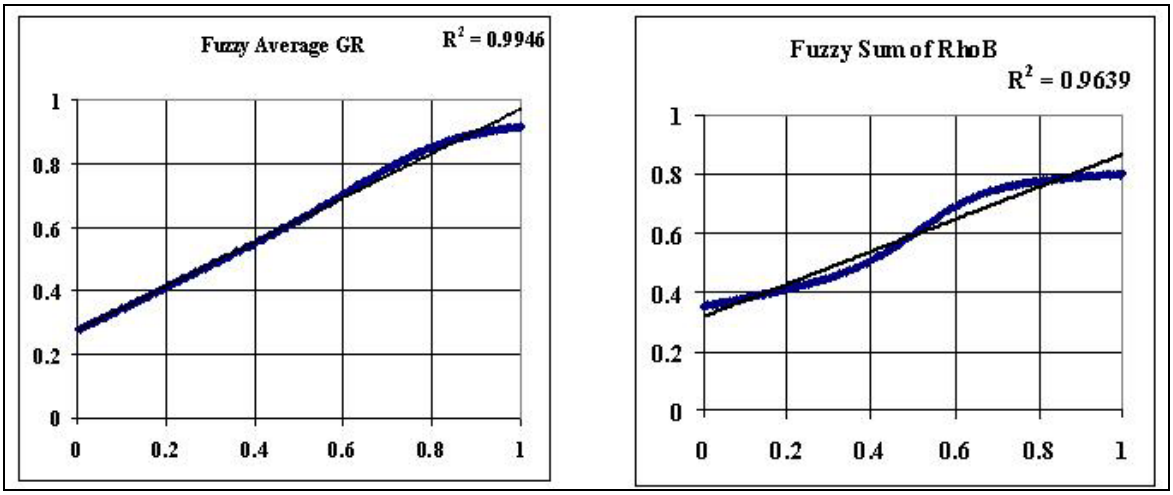

Figure 6. Top ranked fuzzy curves.

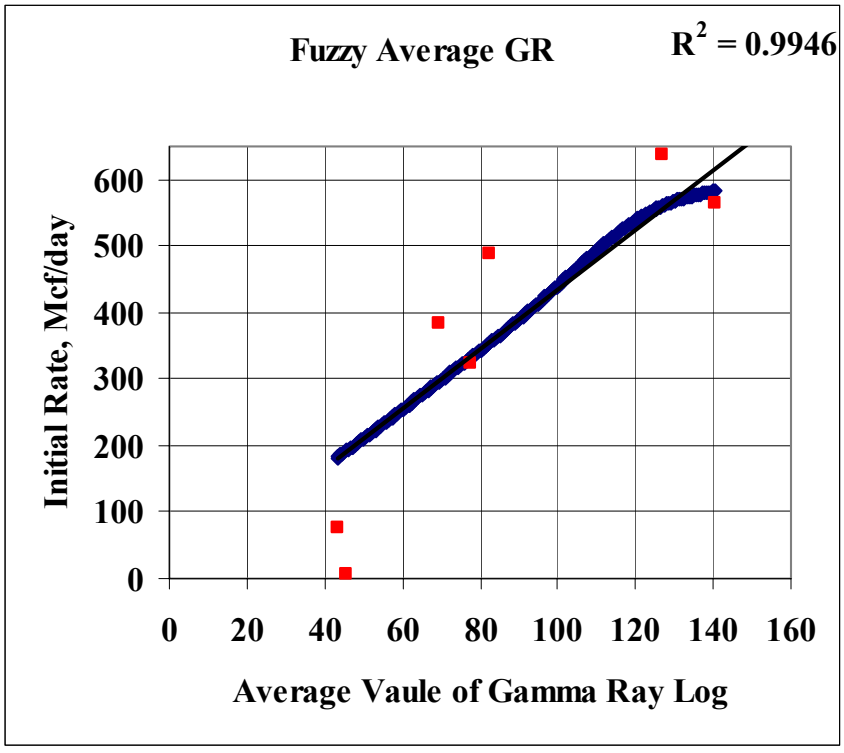

Figure 7. Fuzzy rate versus average gamma ray.

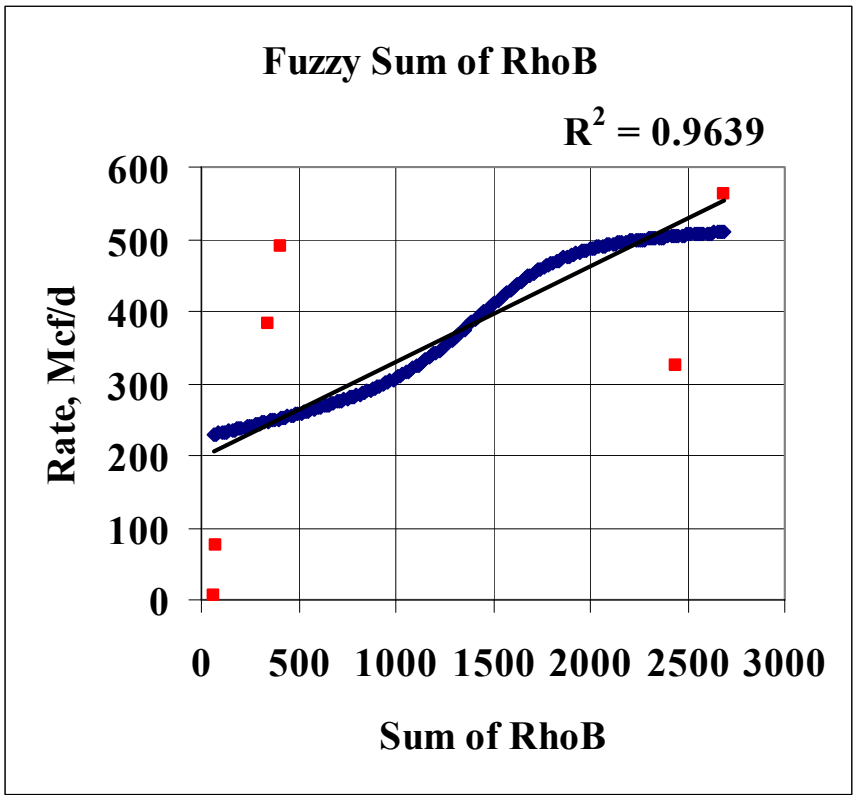

Figure 8. Fuzzy rate vs. Sum of RhoB logs.

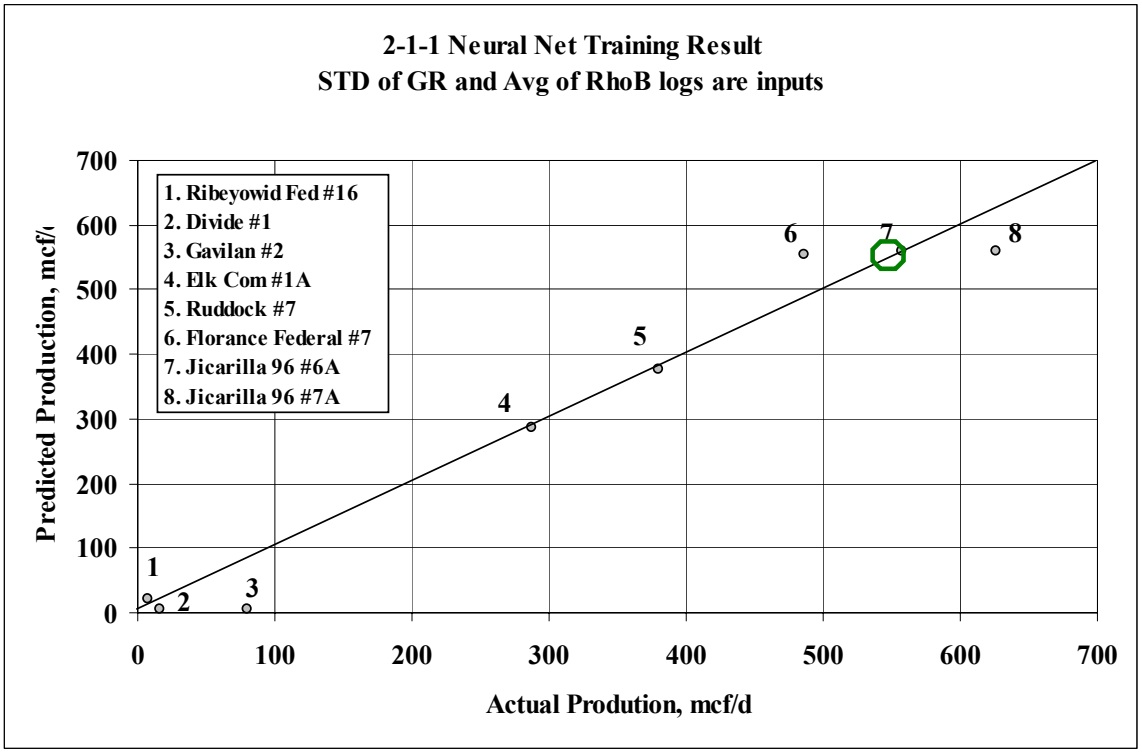

Figure 9 Neural Network training results.

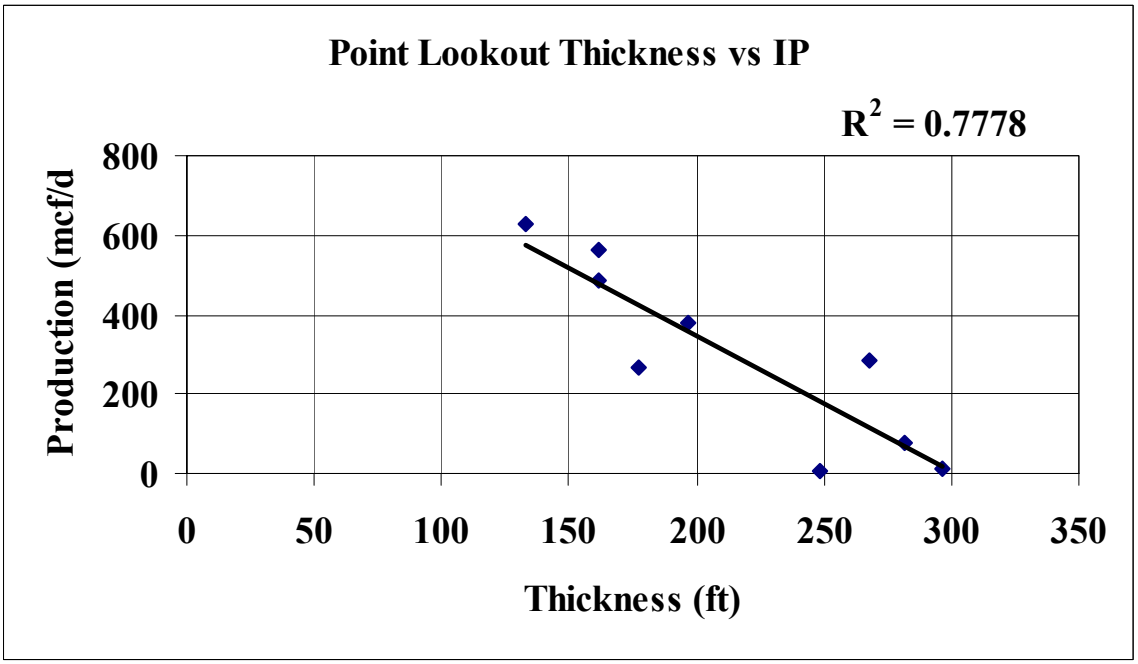

Figure 10 Relationship between initial production and Point Lookout thickness.

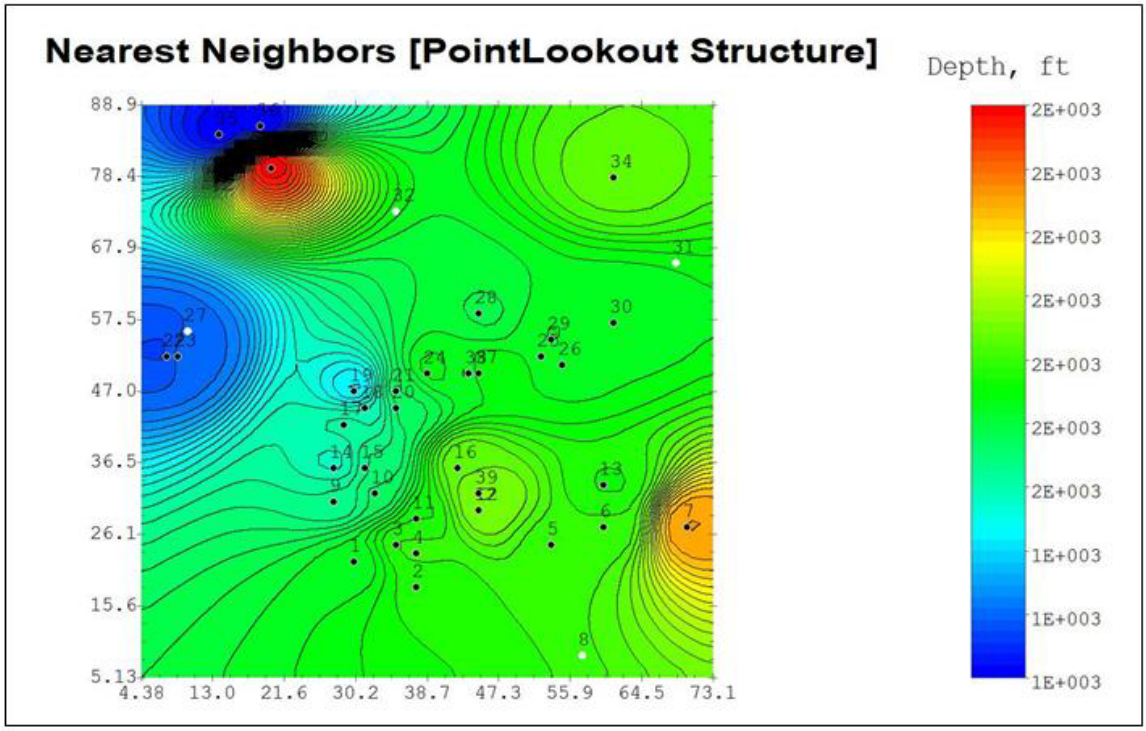

Figure 11 Point Lookout Structure Map.

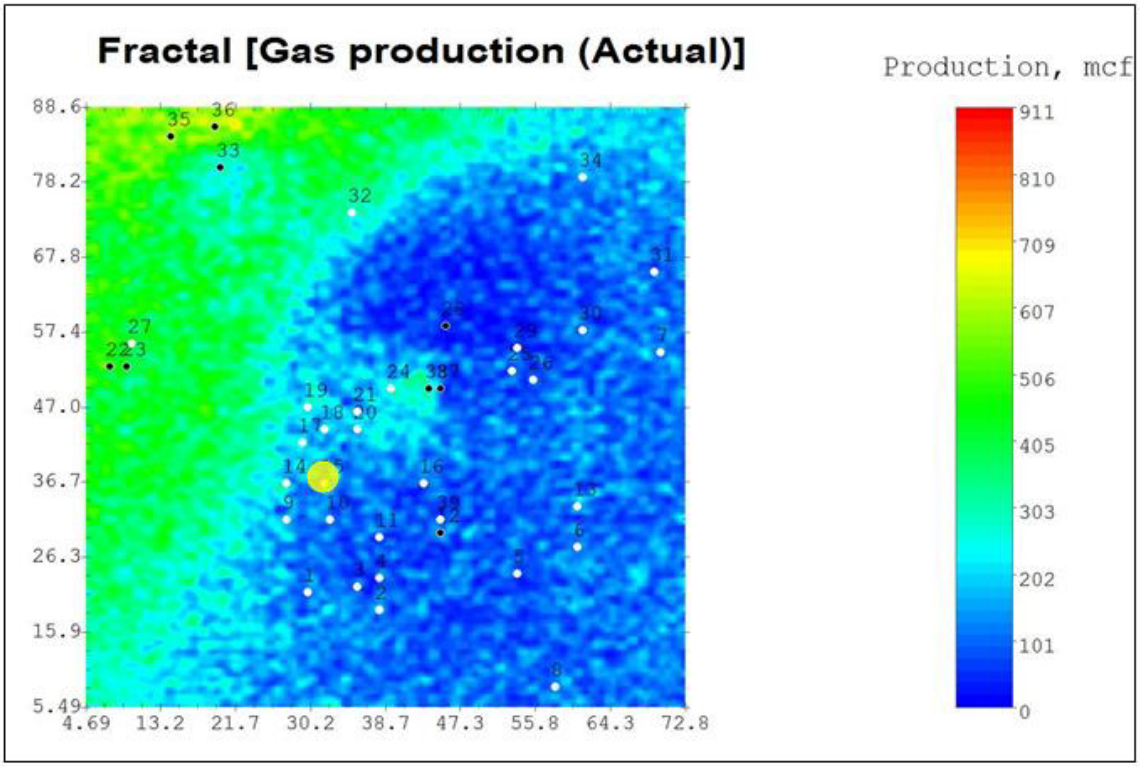

Figure 12 Fractal distribution of Mesaverde production.

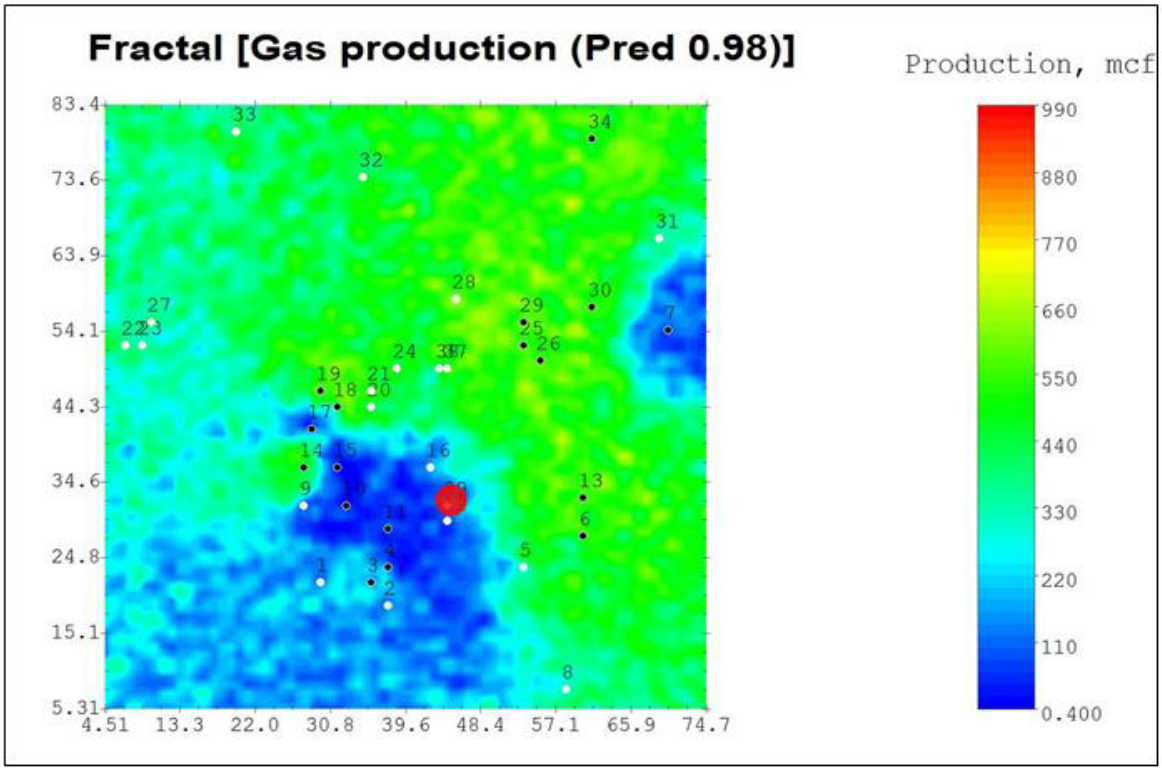

Figure 13 Fractal distribution of predicted Mesaverde production.

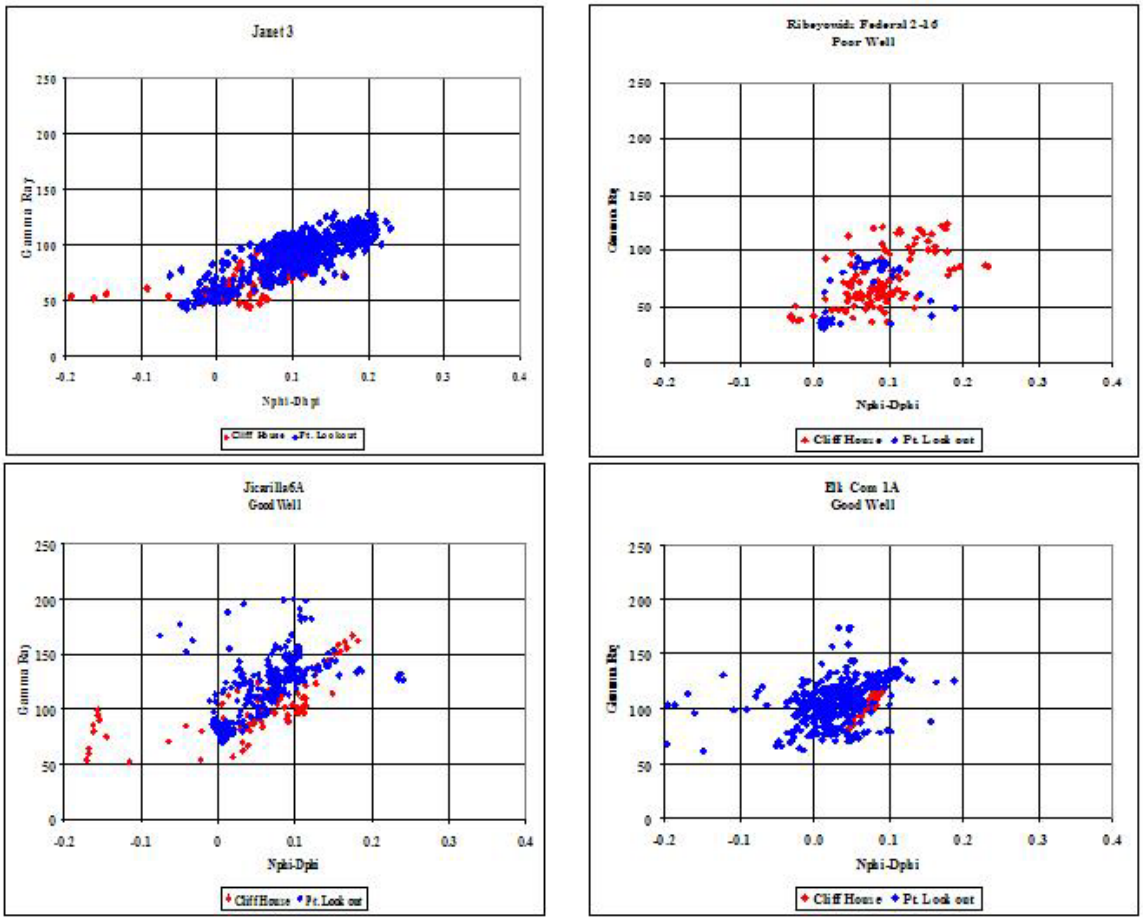

Figure 14 Gamma ray - porosity crossover plots of good wells and bad well plus Janet #3.

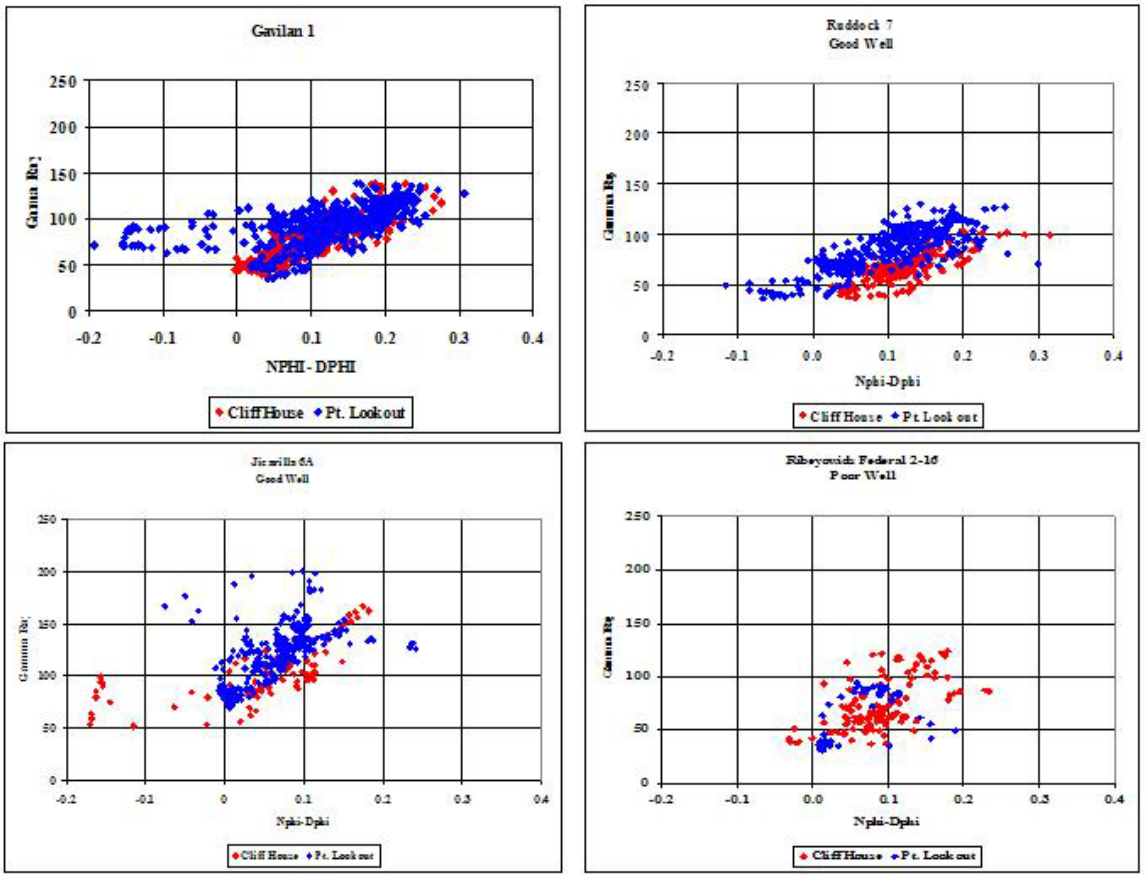

Figure 15 Gamma ray-porosity crossover plots of good wells and bad well plus Gavilan #1.